



# Synthesis of single-walled carbon nanotubes by chemical vapor deposition using sodium chloride support

Jeremy Hor Teong Ooi<sup>a</sup>, Wei-Wen Liu<sup>b</sup>, Venugopal Thota<sup>c</sup>, Abdul Rahman Mohamed<sup>b</sup>, Siang-Piao Chai<sup>a,\*</sup>

<sup>a</sup> School of Engineering, Monash University, Jalan Lagoon Selatan, 46150 Bandar Sunway, Selangor, Malaysia

<sup>b</sup> School of Chemical Engineering, Universiti Sains Malaysia, Engineering Campus, Seri Ampangan, 14300 Nibong Tebal, SPS Pulau Pinang, Malaysia

<sup>c</sup> Welding Alloys (Far East) Sdn. Bhd., 14 & 14A, Jalan Dewani Off Jalan Tampoi, 81100 Johor Bahru, Malaysia

## ARTICLE INFO

### Article history:

Received 26 September 2010

Received in revised form

10 November 2010

Accepted 2 December 2010

Available online 8 December 2010

## ABSTRACT

Bundled single-walled carbon nanotubes (SWCNTs) together with multi-walled carbon nanotubes (MWCNTs) were directly grown on a water-soluble support catalyst that was prepared via sublimation of ferrocene on sodium chloride. The synthesis of nanotubes was carried out at a growth temperature of 700 °C in a combined methane and nitrogen environment of 1:1 volumetric ratio at a total flowrate of 80 ml/min for 1 h in a vertical reactor. Characterization techniques such as scanning electron microscope, transmission electron microscope, thermogravimetric analysis, and Raman spectroscopy were employed to study the carbon deposits. Transmission electron microscope shows the presence of SWCNTs with an average diameter of ca. 1.18 nm on the catalyst. The radial breathing mode (RBM) of Raman for shifts below 350 cm<sup>-1</sup> further confirmed the presence of SWCNTs and the diameters were calculated to be 0.93, 1.36, 1.5 and 1.85 nm.

© 2010 Elsevier B.V. All rights reserved.

## 1. Introduction

Techniques to prepare carbon nanotubes (CNTs) include electro-spinning process, arc discharge, floating catalyst method, and chemical vapor deposition (CVD) [1]. It is known that CVD is one of the most feasible methods of synthesis due to its practicality in terms of relative low cost and ease of scaling up [2]. In CVD, a catalyst placed in a controlled environment inside the furnace forms a platform on which CNTs grow. This catalyst typically comprises of an active metallic component that is chemically blended with a non-metallic support. The metallic component is often a transition metal, with iron, cobalt, and nickel being the notable ones. Other metals such as chromium, platinum, molybdenum, palladium, and copper are used as catalyst promoters [3–5]. The promoter changes the electronic structure of the catalyst, which lowers the activation energy for dissociation. This effectively reduces the growth temperature, and thus enhances the overall performance [3,6].

The non-metallic catalyst support has a role just as important as that of the active metal in synthesizing CNTs abundantly. Essentially a good support must be thermally stable at growth temperature and should not react with the active metal in any way whatsoever under growth condition [7]. Alumina (Al<sub>2</sub>O<sub>3</sub>) and silica (SiO<sub>2</sub>) are the main materials widely used as supports because of their proven potency in synthesizing CNTs [8–11]. Other notable

materials on record include aluminium on oxidized silicon plates and silicon nitride membranes [12,13]. Just very recently, silicon wafers coated with SiO<sub>2</sub> were also studied [14].

To separate CNTs from the catalyst support, the entire piece has to be submerged in a highly concentrated base or acid so that the catalyst would dissolve. This can however be very damaging to the CNTs. The need to reduce pollution certainly does not promote the use of strong acid or any other harmful chemical reagents in the CNT purification process [1,2]. The natural tendency is to search for a viable alternative that simplifies the process while systematically bringing down the cost of production. The use of water soluble catalyst provides a novel solution to this and was pioneered by Szabo et al. [15] using sodium chloride salt as a catalyst support. Subsequently, other researchers also carried out similar studies to scrutinize the capability of different water-soluble catalysts in producing CNTs [1,2,16,17]. The alkali salt is essentially chosen because it is cheap and abundant [2,16]. Just very recently, CNTs were also grown on a potassium fluoride catalyst support [17]. CNTs were reported in all papers with some yielding more than others, but our literature review shows that no paper has ever reported on the formation of SWCNTs over sodium chloride support via methane decomposition.

## 2. Experimental

In this study, 0.15 g of ferrocene (Sigma Aldrich, 98%) was sublimated and deposited on 0.3 g of uncrushed sodium chloride

\* Corresponding author. Tel.: +60 3 55146234; fax: +60 3 55146207.  
E-mail address: [chai.siang.piao@eng.monash.edu.my](mailto:chai.siang.piao@eng.monash.edu.my) (S.-P. Chai).

(NaCl) powder (Sigma Aldrich, 99.5%) to yield Fe/NaCl catalyst. Firstly, the nitrogen flow valve was opened, allowing the inert gas to purge the whole unit at 40 ml/min for 15 min. After purging, the furnace was switched on and the temperature was brought up to 700 °C in the continuous flow of nitrogen gas. Upon achieving this, methane gas was introduced into the system with a flowrate of 40 ml/min. There was a total of 80 ml/min of mixed nitrogen and methane gases at 1:1 volumetric ratio flowing in the path of the vertical reactor. The temperature at the ferrocene bed was recorded to be approximately 130 °C while the reactor temperature was 700 °C. The reaction was carried out for 1 h. Fig. 1 shows a schematic of the experimental set-up.

After CVD of methane, the carbon deposits were analyzed using scanning electron microscopy (SEM) (FEI Quanta 200 FEG-SEM) and transmission electron microscopy (TEM) (Philips CM12). Thermogravimetric analysis (TGA) was also carried out with TGA-Q50 from ambient temperature to 750 °C. The sample was loaded into the TGA and heated from room temperature to 110 °C in nitrogen atmosphere. Having achieved this, the TGA was left in isothermal condition for 2 min before purified air was channeled into the furnace. The sample was then further heated up to 850 °C and was maintained in isothermal condition for 1 min before finally initiating the cooling process. The weight loss with temperature, corresponding to the oxidation of deposited carbon, determines the amount of carbon produced by the catalyst. Raman scattering was also carried out on the sample using the Renishaw inVia Raman microscope to characterize the degree of graphitization and the types of carbon present. In order to verify the composition of the catalyst, the sample was also subjected to X-Ray Diffraction (XRD) analysis using the D8 Advance X-Ray

Diffractionmeter-Bruker AXS, which emits  $\text{CuK}\alpha$  radiation through a graphite secondary beam monochromator with  $2\theta$  ranging from 10° to 80°.

### 3. Results and discussion

Fig. 2(a–c) shows the SEM images of CNTs grown on the Fe/NaCl catalyst after CVD of methane at 700 °C. On each grain, there were bright spots and black spots randomly scattered all over. The black areas are carbon settlements where CNTs could be located. After zooming in further on the black area with higher magnification, long tubular structures of different diameters were observed. Other structures such as amorphous carbon and carbon encapsulated iron particles were also spotted amongst the graphitized tubular structures. Though easily located all over the sample, the yield of CNTs did not seem high. Fig. 3(a and b) shows the TEM images of CNTs and it revealed the morphology of the as-grown CNTs to be bundled SWCNTs with an average diameter of ca. 1.18 nm. The nature of SWCNTs forming in bundles could be attributed to the intertube van der Waals' attraction and the instability of a single strand of SWCNT standing on its own [18].

The Raman spectrum of the carbon deposit is shown in Fig. 4(a). A D-band at  $1339.55\text{ cm}^{-1}$  and a G-band at  $1588.12\text{ cm}^{-1}$  were observed. The G-band is a characteristic feature of the graphitic layers and corresponds to the tangential vibration of the carbon atoms while the D-band reflects defective scattering, which breaks the basic symmetry of the graphene sheet [19]. There is a standard intensity ratio of D-band to G-band ( $I_D/I_G$ ) to measure the bulk constitution of a sample and for this sample the ratio is 0.672, indicating a high degree of graphitization. This aside, the Radial Breathing Mode (RBM), which constitutes the shifts ranging from  $350\text{ cm}^{-1}$  and below also provides good insight into the composition of the catalyst from a different perspective (Fig. 4(b)). It is a commonly used technique to identify and evaluate the diameter of SWCNTs. Analysis of Fe/NaCl after CVD in methane at 700 °C has shown significant peaks that consolidate the authenticity of the

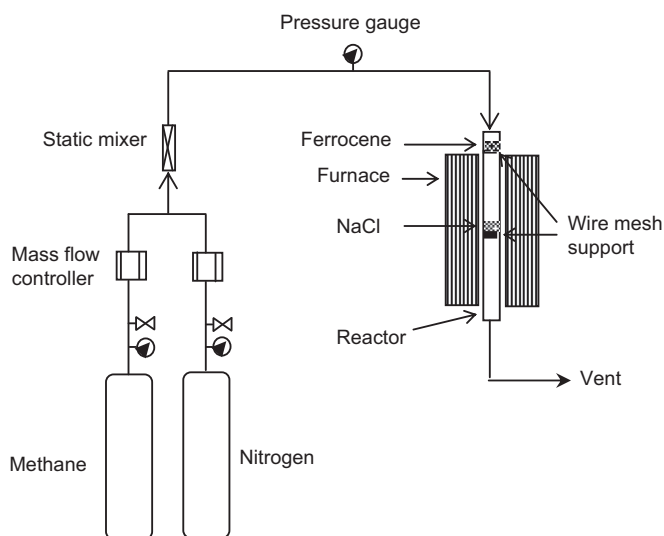


Fig. 1. Schematic diagram of the experimental set-up.

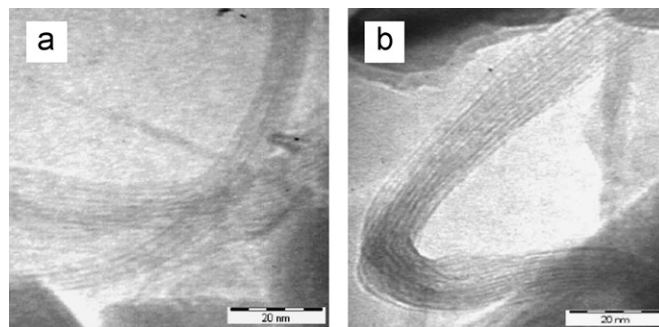


Fig. 3. (a and b) TEM images showing SWCNT bundles.

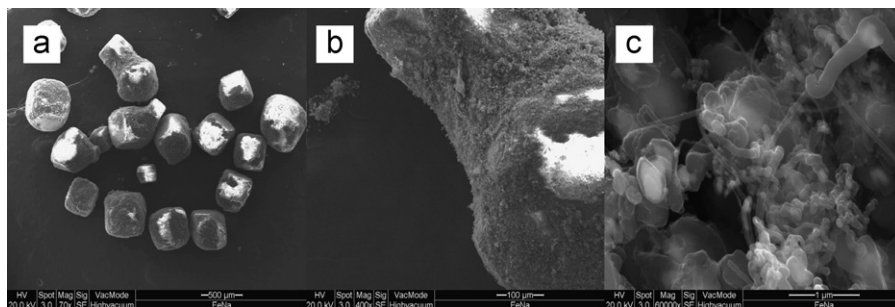


Fig. 2. (a–c) SEM images of Fe/NaCl after CVD of methane at different magnification levels.

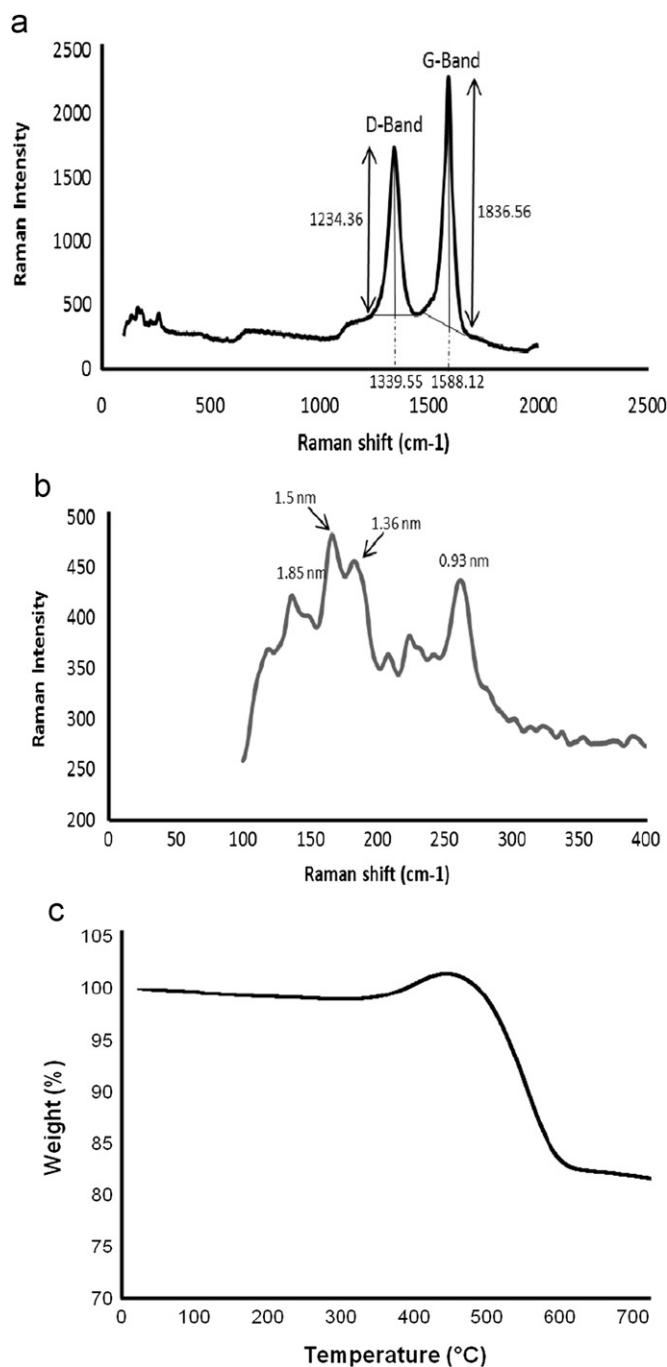


Fig. 4. (a) Raman spectrum, (b) Radial Breathing Mode, and (c) TGA plot of Fe/NaCl after CVD of methane.

presence of SWCNTs also shown in the TEM image. There are four discernible peaks with the first one corresponding to  $136.56 \text{ cm}^{-1}$  and the second at  $165.94 \text{ cm}^{-1}$ . The third is spotted at  $182.28 \text{ cm}^{-1}$  and the last is located at  $261.71 \text{ cm}^{-1}$ . By using the expression and applying experimental constants of A and B with corresponding values of 234 and  $10 \text{ cm}^{-1}$ , respectively, as reported in Ref. [20], the diameters of the SWCNTs were calculated to be 1.85, 1.5, 1.36, and 0.93 nm.

Fig. 4(c) shows a TGA plot of the Fe/NaCl catalyst after CVD of methane. At the initial stage of heating from ambient temperature to 400 °C, there was a slight drop in weight and this coincides with the removal of absorbed water in the sample and oxidation of the disoriented carbon [21–23]. At 400 °C, the weight increased and

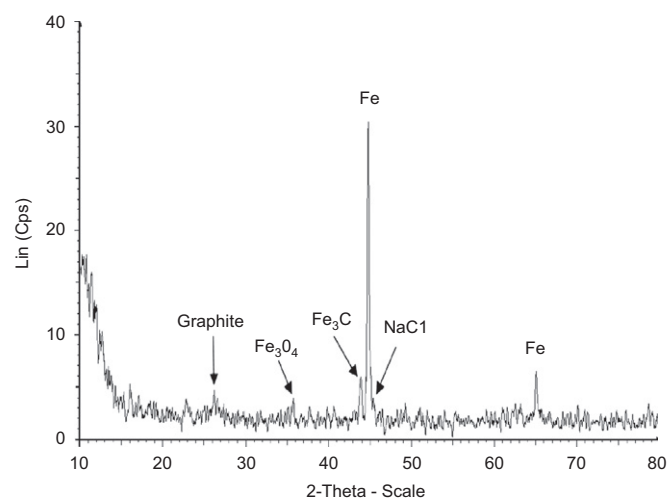


Fig. 5. XRD plot of Fe/NaCl after CVD of methane.

surpassed the 100% mark. At this point, it is believed that iron reacted with oxygen from the purified air to form iron oxide. This occurrence was observed because oxide was not a part of the initial weight measured. The line plunged steeply as heating reached 450 °C. Until about 600 °C, there was a 20% drop in weight. This is attributed to carbon oxidation [24]. At this point, TGA verified the presence of carbon or specifically the presence of CNTs because amorphous carbon was oxidized earlier between 240 and 400 °C [21–23].

Fig. 5 shows the XRD result. There are multiple distinct peaks ranging from  $2\theta = 10^\circ$  to  $80^\circ$ . Graphite is located at  $2\theta = 26^\circ$  and this peak corresponds to aligned and structured carbon, which includes CNTs [25,26]. The peak at  $2\theta = 45.5^\circ$  is unique to NaCl [27]. Iron is in great abundance as signified by the high peak at  $2\theta = 45^\circ$ . Iron carbide formed at  $2\theta = 43^\circ$  as a result of carbon dissolution and saturation in iron [28]. Its significance is elucidated in the succeeding brief description of the growth mechanism. The three fundamental principles of the CVD method in synthesizing CNTs are in the order of decomposition, diffusion, and precipitation [29]. Upon introduction of reaction gas, the molecules are adsorbed on the iron particle surface. Decomposition of the carbon-containing molecules then takes place on the iron surface. What follows is the diffusion of free carbon atoms through the iron particle due to a difference in concentration gradient of carbon atoms. Upon saturation, carbon reacts with iron to form iron carbide. Finally, the precipitation of the diffused free carbon atoms takes place at the iron–NaCl interface to complete the initial process of CNT growth [16]. Thereafter, the hemifullerene cap formed on the partially carbon-coated particle lifts off and additional carbon atoms are continuously added to the edge of the cap, forming a hollow tube that grows away from the particle [30]. In short, with the formation of iron carbide, CNTs grows subsequently. Thus the presence of iron carbide is a positive inference.

#### 4. Conclusions

It is demonstrated for the first time that SWCNTs were grown from methane CVD on NaCl support. SEM showed the presence of CNTs, albeit low in abundance. TGA confirmed that CNTs were present with a yield of about 20%. Raman spectroscopy gave a good indication of CNTs with a high G-band peak and an encouraging intensity ratio of  $I_D/I_G$  of 0.672. The RBM showed the presence of SWCNTs with diameters ranging from 0.93 to 1.85 nm. TEM

verified the presence of SWCNTs with an average diameter of ca. 1.18 nm, consistent with the values presented by Raman.

## Acknowledgements

The authors would like to thank the funding provided by the Monash University through the Monash Internal Seed Fund (A/C no: E-9-09) and the Ministry of Higher Education Malaysia (MOHE) through the Fundamental Research Grant Scheme (FRGS) (Ref no. FRGS/2/2010/TK/MUSM/03/4).

## References

- [1] M. Jia, Y. Zhang, *Mater. Lett.* 63 (2009) 2111.
- [2] J. Geng, I. Kinloch, C. Singh, V. Golovko, B. Johnson, M. Shaffer, Y. Li, A. Windle, *J. Phys. Chem.* 109 (2005) 16665.
- [3] C.J. Lee, J. Park, J.M. Kim, Y. Huh, J.Y. Lee, K.S. No, *Chem. Phys. Lett.* 327 (2000) 277.
- [4] W.M. Yeoh, K.Y. Lee, S.P. Chai, K.T. Lee, A.R. Mohamed, *J. Alloys Compd.* 493 (2010) 539.
- [5] S.P. Chai, S.H.S. Zein, A.R. Mohamed, *Chem. Phys. Lett.* 426 (2006) 345.
- [6] A.R. Harutyunyan, B.K. Pradhan, U.J. Kim, G. Chen, P.C. Eklund, *Nano Lett.* 2 (2002) 525.
- [7] R.L. Vander Wal, T.M. Tichich, V.E. Curtis, *Carbon* 39 (2001) 2277.
- [8] R. Engel-Herbert, H. Pforte, T. Hesjedal, *Mater. Lett.* 61 (2007) 2589.
- [9] D. Hanifeh Toubestani, M. Ghoranneviss, A. Mahmoodi, M. Rahbar Zareh, *Macromol. Symp.* 287 (2010) 143.
- [10] N. Li, X. Wang, S. Derrouiche, G.L. Haller, L.D. Pfefferle, *ACS Nano* 4 (2010) 1759.
- [11] P. Zarabadi-Poor, A. Badiei, A.A. Yousefi, B.D. Fahlman, A. Abbasi, *Catal. Today* 150 (2010) 100.
- [12] N. Singh, R. Gargate, D. Banerjee, A. Patil, *Proc. SPIE Int. Soc. Opt. Eng.* (2009) 731809.
- [13] X.G. Sun, L. Cheng, G.P. Du, *J. Syn. Crys.* 38 (2009) 1114.
- [14] M.R. Aguiar, C. Verissimo, A.C.S. Ramos, S.A. Moshkalev, J.W. Swart, *J. Nanosci. Nanotechnol.* 9 (2009) 4143.
- [15] A. Szabó, D. Méhn, Z. Kónya, A. Fonseca, J.B. Nagy, *Phys. Chem. Commun.* 6 (2003) 40.
- [16] A. Eftekhari, P. Jafarkhani, F. Moztarzadeh, *Carbon* 44 (2006) 1343.
- [17] S. Manafi, S. Joughehdoust, S.H. Badiee, *Int. J. Nanomanuf.* 1–2 (2010) 100.
- [18] M. Krishna Kumar, A. Leela Mohana Reddy, S. Ramaprabhu, *Sensors Actuators B Chem.* 130 (2008) 653.
- [19] S. Costa, E. Borowiak-Palen, M. Kruszynska, A. Bachmatiuk, R.K. Kaleńczuk, *Mater. Sci. Pol.* 26 (2008) 433.
- [20] M. Milnera, J. Kürti, M. Hulman, H. Kuzmany, *Phys. Rev. Lett.* 84 (2000) 1324.
- [21] E. Dervishi, Z. Li, A.R. Biris, D. Lupu, S. Trigwell, A.S. Biris, *Chem. Mater.* 19 (2006) 179.
- [22] R.B. Mathur, S. Seth, C. Lal, R. Rao, B.P. Singh, T.L. Dhami, A.M. Rao, *Carbon* 45 (2007) 132.
- [23] M. Khavarian, S.P. Chai, S.H. Tan, A.R. Mohamed, *Nano* 4 (2009) 359.
- [24] D. Bom, R. Andrews, D. Jacques, J. Anthony, B. Chen, M.S. Meier, J.P. Selegue, *Nano Lett.* 2 (2002) 615.
- [25] H.J. Choi, G.B. Kwon, G.Y. Lee, D.H. Bae, *Scr. Mater.* 59 (2008) 360.
- [26] B. Liu, H.Y. Li, L. Die, X.H. Zhang, Z. Fan, J.H. Chen, *J. Power Sources* 186 (2009) 62.
- [27] X. Jiang, X. Tian, Z. Fan, *Mater. Res. Bull.* 43 (2008) 343.
- [28] J. Yang, J. Ma, W. Liu, Q. Bi, Q. Xue, *Scr. Mater.* 58 (2008) 1074.
- [29] Y. Zhang, X. Sun, *Adv. Mater.* 19 (2007) 961.
- [30] P. Nikolaev, M. Bronikowski, R. Bradley, F. Rohmund, D. Colbert, K. Smith, *Chem. Phys. Lett.* 313 (1999) 91.